Surfing on Turbulence: A Strategy for Planktonic Navigation

Rémi Monthiller, Aurore Loisy, Mimi A. R. Koehl, Benjamin Favier, and Christophe Eloy

Surfing on turbulence

Rmi Monthiller,[1] Aurore Loisy,[1] Mimi A. R. Koehl,[2] Benjamin Favier,[1] and Christophe Eloy[1]

[1] *Aix Marseille Univ, CNRS, Centrale Marseille, IRPHE, Marseille, France*
[2] *Department of Integrative Biology, University of California, Berkeley, CA 94720-3140, USA*

In marine plankton, many swimming species can perceive their environment with flow sensors. Can they use this flow information to travel faster in turbulence? To address this question, we consider plankters swimming at constant speed, whose goal is to move upwards. We propose a robust analytical behavior that allows plankters to choose a swimming direction according to the local flow gradients. We show numerically that such plankters can "surf" on turbulence and reach net vertical speeds up to twice their swimming speed. This new physics-based model suggests that planktonic organisms can exploit turbulence features for navigation.

Plankton are small organisms drifting in oceans. While they are carried by the ambient turbulent flow, many can swim and are equipped with hair-like mechanosensory organelles used to sense flows relative to their bodies, i.e. velocity gradients [1–4]. Besides, many can sense gravity or light [5–7], both indicating which direction is up. Here we focus on a planktonic navigation problem in turbulence: can motile planktonic organisms use local hydrodynamic signals to travel faster than their swimming speed along the vertical direction?

Vertical migration is an important task for many types of plankton. For instance, copepods are abundant millimetric crustaceans that move upwards to food-rich surface waters at night and downwards away from visual predators during the day [5, 8]. Various planktonic larvae migrate up or down into currents at particular depths that transport the larvae horizontally [9–11]. Some larvae, when ready to settle, sink or swim downwards in response to chemical cues [12] or mechanical stimuli due to turbulence [13–16].

The navigation task faced by plankters has two features: (1) plankters only sense local flow information; and (2) plankters only sense velocity gradients, not flow velocities. This makes planktonic navigation different from the Zermelo's navigation problem [17] (where agents sense the full velocity field) and the bird soaring problem [18, 19] (where birds sense the vertical flow velocity).

Problems of planktonic navigation have been recently approached using reinforcement learning [20–25]. These studies showed that strategies based on local gradients can be learned in simple flows. Training a microswimmer in unsteady 3D turbulence remains however challenging [23, 24]. Besides, the strategies learned are not necessarily optimal nor easily interpretable.

Different models of zooplankton in turbulence have explored the consequences of various behaviors [26, 27]. For example, models of slowly-swimming planktonic larvae of different shapes in turbulent flow [28–30] or in shear [31]have shown how steady swimming or sinking, or behavioral responses to chemical or hydrodynamic cues can affect where they are transported by the ambient flow. A model of copepods finding patches of prey in turbulence

included sensory cues, but not transport by ambient water motion [32]. These data-based models are however purely empirical.

In this Letter we propose an approach based on physical principles. We model the navigation problem of going upwards and we derive an approximate solution, within well-defined hypotheses, where the response (preferred swimming direction) is an analytic function of the environmental signal (local velocity gradient). This behavior can be interpreted as "surfing" on the flow (Fig. 1): to exploit upward fluid motions, the plankter chooses a swimming direction by assuming that the flow is locally steady and linear.

We consider a plankter in homogeneous, isotropic turbulence. Its task is to go as fast as possible in a target direction, which is chosen to be $\hat{\boldsymbol{z}}$, the vertical, without loss of generality. We model the plankter as an active particle with position $\boldsymbol{X}(t)$, swimming in direction $\hat{\boldsymbol{p}}(t)$ at constant swimming speed V_{swim} in a 3D flow velocity field $\boldsymbol{u}(\boldsymbol{x}, t)$. The plankter is assumed to be inertialess, neutrally buoyant, and small compared to the Kolmogorov scale η (the scale of the smallest turbulent flow features [33]). It actively controls its orientation by choosing a direction $\hat{\boldsymbol{n}}$. We start by assuming that the swimming
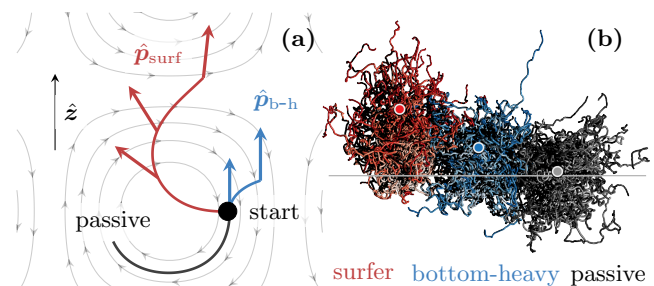

FIG. 1. Plankters can exploit velocity gradients to "surf" on the flow: (a) 2D Taylor-Green vortex flow; (b) 3D turbulent flow. We compare the trajectories of surfers (red) to those of bottom-heavy swimmers (blue), which always swim upwards. We also show trajectories of passive particles (black). In (a), arrows show the swimming direction. In (b), the gray line shows the depth of the initial positions and circles show the average final vertical position for the same turbulent flow.

direction $\hat{\boldsymbol{p}}$ is always aligned with this chosen direction $\hat{\boldsymbol{n}}$. This corresponds to the limit of instantaneous reorientation (the effect of a finite reorientation time will be addressed below). Under these assumptions, the equations of motion are

$$\frac{d\boldsymbol{X}}{dt} = \boldsymbol{u}(\boldsymbol{X}, t) + V_{\text{swim}}\,\hat{\boldsymbol{p}}, \quad (1\text{a})$$

$$\hat{\boldsymbol{p}}(t) = \hat{\boldsymbol{n}}(t). \quad (1\text{b})$$

We assume that the plankter senses the local flow velocity gradient $\boldsymbol{\nabla}\boldsymbol{u}$ and the vertical direction $\hat{\boldsymbol{z}}$. It responds to this information by choosing a direction $\hat{\boldsymbol{n}}(\boldsymbol{\nabla}\boldsymbol{u}, \hat{\boldsymbol{z}})$, without any memory. The metric used to quantify the performance of the plankters is the effective velocity, V_{eff}, defined as the long-time average velocity along $\hat{\boldsymbol{z}}$

$$V_{\text{eff}} = \lim_{T\to\infty} \frac{\boldsymbol{X}(T) - \boldsymbol{X}(0)}{T} \cdot \hat{\boldsymbol{z}}. \quad (2)$$

In the language of control theory (resp. reinforcement learning), $\hat{\boldsymbol{n}}(\boldsymbol{\nabla}\boldsymbol{u}, \hat{\boldsymbol{z}})$ is the control (resp. policy) and V_{eff} is the objective function (resp. return).

Using a Taylor expansion of $\boldsymbol{u}(\boldsymbol{x}, t)$ in the neighborhood of the current time t_0 and position $\boldsymbol{X}_0 = \boldsymbol{X}(t_0)$, the velocity field can be approximated as

$$\boldsymbol{u}(\boldsymbol{x}, \tau) \approx \boldsymbol{u}_0 + (\boldsymbol{\nabla}\boldsymbol{u})_0 \cdot (\boldsymbol{x} - \boldsymbol{X}_0) + \left(\frac{\partial\boldsymbol{u}}{\partial t}\right)_0 (\tau - t_0), \quad (3)$$

where the subscript 0 indicates a variable evaluated at time t_0 and location $\boldsymbol{X}_0$ (e.g., $\boldsymbol{u}_0 = \boldsymbol{u}(\boldsymbol{X}_0, t_0)$). Inserting approximation (3) into Eqs. (1) and integrating [34], one can show that the displacement along $\hat{\boldsymbol{z}}$ between time t_0 and $t_0 + \tau$ is maximized when

$$\boldsymbol{n}(t_0 + t) = \left[\exp\left((\tau - t)(\boldsymbol{\nabla}\boldsymbol{u})_0\right)\right]^T \cdot \hat{\boldsymbol{z}}, \quad (4)$$

with $0 \le t \le \tau$, $\exp(\cdot)$ the matrix exponential, and $[\cdot]^T$ denoting the transpose. For a plankter continuously sensing the flow, we can set $t = 0$ and drop the subscript 0. After normalization, the preferred direction of the surfing strategy is thus

$$\hat{\boldsymbol{n}}_{\text{surf}} = \frac{\boldsymbol{n}_{\text{surf}}}{|\boldsymbol{n}_{\text{surf}}|}, \quad \text{with } \boldsymbol{n}_{\text{surf}} = \left[\exp\left(\tau\boldsymbol{\nabla}\boldsymbol{u}\right)\right]^T \cdot \hat{\boldsymbol{z}}, \quad (5)$$

with the time horizon τ a free parameter of this surfing strategy.

The fully-turbulent flow that models the plankter environment is obtained from the Johns Hopkins Turbulence Database [35, 36]. It is a direct numerical simulation of a 3D homogeneous isotropic turbulent flow with $Re_\lambda = 418$. The Lagrangian equations of plankter motion, Eqs. (1), are integrated with an in-house open-source code, SHELD0N [37], using a 4th-order temporal Runge-Kutta scheme and a 6th-order spatial interpolation scheme.
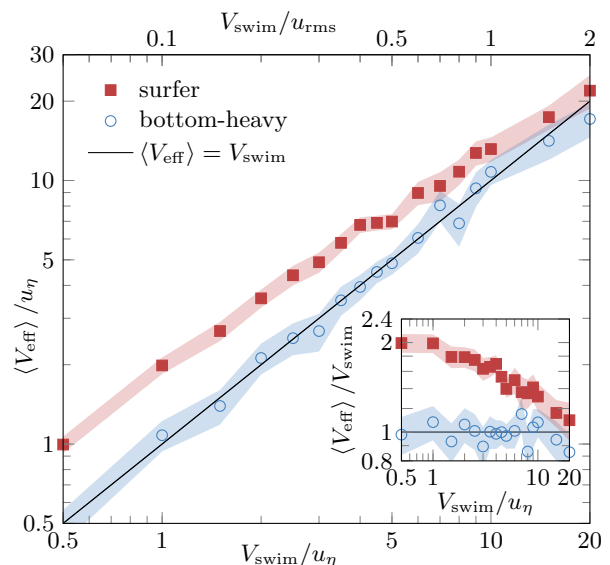

FIG. 2. Effective upward velocity (V_{eff}, defined by Eq. (2)) as a function of the swimming velocity (V_{swim}) for a surfer ($\hat{\boldsymbol{n}} = \hat{\boldsymbol{n}}_{\text{surf}}$ with optimal time horizon $\tau = \tau^*$) and for a bottom-heavy swimmer ($\hat{\boldsymbol{n}} = \hat{\boldsymbol{z}}$), here assuming instantaneous reorientation time (Eq. 1). Velocities are normalized either by the Kolmogorov velocity (u_η, Eq. (6)) (bottom x-axis) or by the root-mean-square velocity u_{rms} (top x-axis). The inset presents the same data where the effective upward velocity is normalized by the swimming velocity. The solid line represents $V_{\text{eff}} = V_{\text{swim}}$. Shaded areas correspond to 95% confidence intervals.

In a turbulent flow, the smallest flow features are described by the Kolmogorov time τ_η and Kolmogorov velocity u_η

$$\tau_\eta = (\nu/\epsilon)^{1/2}, \quad u_\eta = (\nu\epsilon)^{1/4}, \quad (6)$$

with ν the kinematic viscosity and ϵ the average dissipation rate [33]. The largest flow features are characterized by the large-eddy turnover time T_L and the root-mean-square velocity u_{rms}, with $T_L \approx 47\tau_\eta$ and $u_{\text{rms}} \approx 10u_\eta$ here. Unless mentioned otherwise, the performance is evaluated after a time $T \approx 5T_L$, using Eq. (2), and averaged over N plankters with random initial positions. Averaged quantities are noted $\langle\cdot\rangle$. N varies from 10 for $V_{\text{swim}} = 20u_\eta$ to 16384 for $V_{\text{swim}} = u_\eta/2$ to ensure similar uncertainties on performance.

We now assess the performance of surfers, which actively choose a preferred direction $\hat{\boldsymbol{n}} = \hat{\boldsymbol{n}}_{\text{surf}}$, given by Eq. (5). For that purpose, we compare them to bottom-heavy swimmers, which passively align upwards, that is $\hat{\boldsymbol{n}} = \hat{\boldsymbol{z}}$. In Fig. 2, we show that surfers can reach effective speeds, V_{eff}, as large as twice their swimming speed when $V_{\text{swim}} \lesssim u_\eta$. They systematically outperform bottom-heavy swimmers, whose performance is $V_{\text{eff}} = V_{\text{swim}}$ in the limit of instantaneous reorientation (Eq. 1b). This is because turbulence acts as a random noise of zero mean
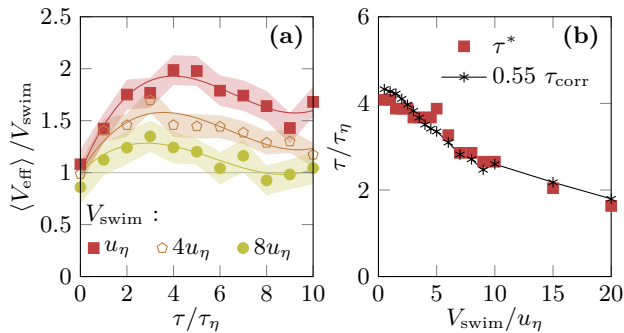
FIG. 3. Influence of the time horizon on the surfing strategy. (a) Effect of the time horizon (τ, Eq. (5)) on the effective velocity ($V_{\rm eff}$, Eq. (2)), for different swimming velocities $V_{\rm swim}$. Shaded area represents the 95% confidence interval. Solid lines represent a fit with Chebyshev polynomials of degree 3. (b) Correlation time $\tau_{\rm corr}$, defined in Eq. (7), and optimal time horizon τ^* as a function of swimming velocity (τ^* is evaluated using the fitted polynomial).
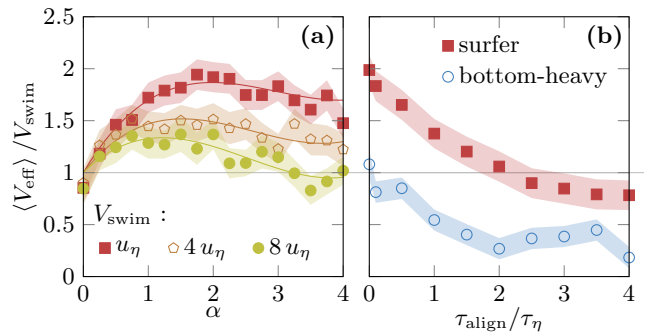

FIG. 4. (a) Performance ($V_{\rm eff}/V_{\rm swim}$) of surfers using a time dependent τ as a function of the dimensionless constant α (Eq. (8)) for different swimming velocities $V_{\rm swim}$. Solid lines represent a fit with Chebyshev polynomials of degree 3. (b) $V_{\rm eff}/V_{\rm swim}$ of surfers and bottom-heavy swimmers as a function of the reorientation time $\tau_{\rm align}$. $V_{\rm swim} = u_\eta$. Shaded area represents the 95% confidence interval.

for bottom-heavy swimmers. In contrast, surfers can exploit the turbulent flow by biasing the sampling of vertical flow velocities [34]. This shows that sensing flow gradients is beneficial for navigation in turbulence and that surfing allows to exploit this information.

To determine the optimal value of the time horizon τ^*, we look numerically for the best performance when τ varies in the range $[0, 10\tau_\eta]$ (Fig. 3a). For all swimming velocities $V_{\rm swim}$, the performance $V_{\rm eff}$ has a clear velocity-dependent maximum at $\tau^*(V_{\rm swim}) = O(\tau_\eta)$. When $\tau \ll \tau_\eta$, surfers do not use gradient sensing and swim upwards (see Eq. 5). Acting as bottom-heavy swimmers, their performance is $V_{\rm eff} = V_{\rm swim}$. When $\tau \gg \tau_\eta$, the steady linear approximation of the flow, given in Eq. (3), breaks down and the planned route becomes irrelevant. The optimal value τ^* can thus be interpreted as the time interval over which the steady linear approximation of the flow is reasonable. For $V_{\rm swim} = u_\eta$, the optimal time horizon is $\tau^* \approx 4\tau_\eta$. Although our results are based on a single simulation at large Reynolds number, we expect our conclusions to be qualitatively independent of Re, because of the universality of turbulence at small scale in the limit of large Re [33].

The relative surfer performance, $V_{\rm eff}/V_{\rm swim}$, decreases as the swimming speed increases (Fig. 2). This is because the correlation time of the flow gradients measured by a plankter decreases as $V_{\rm swim}$ increases. In other words, when plankters swim faster, the surrounding flow changes faster. Therefore, τ^* and $V_{\rm eff}$ decrease with swimming speed. Supported by this observation, we hypothesize that the optimal time horizon τ^* scales as a correlation time $\tau_{\rm corr}$. We define $\tau_{\rm corr}$ as the integral of the period, $2\pi/\omega$, weighted by the spectrum of $\mathrm{Tr}([\boldsymbol{\nabla u}]^2)^{1/2}$ mea-

sured along trajectories of plankters

$$\tau_{\rm corr}(V_{\rm swim}) = \frac{\int \langle I(\omega) \rangle \frac{2\pi}{\omega} \, d\omega}{\int \langle I(\omega) \rangle \, d\omega}, \tag{7}$$

where $I(\omega)$ is the temporal modulus of the Fourier transform of $\mathrm{Tr}([\boldsymbol{\nabla u}]^2)^{1/2}$ and depends on the swimming velocity. Figure 3b shows that, up to a multiplicative constant, $\tau_{\rm corr}$ is a good predictor of the optimal time horizon with $\tau^* \approx 0.55\tau_{\rm corr}$. The choice of I in Eq. 7 is not unique, but other invariants of the velocity gradient yield similar results [34].

We now discuss the applicability of the surfing behavior to more realistic situations relevant to planktonic navigation. First, the turbulence intensity of plankton environments fluctuates on short time scales [38]. This may appear as a problem since surfers need to evaluate the value of τ_η of their local environment to choose the optimal time horizon τ^*. But in practice τ_η can be estimated from the velocity gradient itself since $\tau_\eta \sim 1/|\mathrm{sym}\,(\boldsymbol{\nabla u})|$ where $|.|$ is the Frobenius norm [39]. This suggests a refinement of the surfing strategy where τ in Eq. (5) is replaced by

$$\tau = \frac{\alpha}{|\mathrm{sym}\,(\boldsymbol{\nabla u})|}, \tag{8}$$

with α a dimensionless parameter, which can be viewed as a dimensionless time horizon. In Fig. 4a, we show that surfers using this modified strategy perform as well as surfers with a constant time horizon τ. For $V_{\rm swim} = u_\eta$, the optimal value of parameter α is $\alpha^* \approx 2$. This value is presumably independent of the turbulence intensity.

Second, sensing and motor control of real organisms may be subject to noise. We show in Supplemental Material [34] that the surfing strategy is robust to noisy measures of $\hat{\boldsymbol{z}}$ or $\boldsymbol{\nabla u}$ and to noisy control of its preferred direction $\hat{\boldsymbol{n}}$: for all noise sources, the performance remains practically unchanged for noise up to 25%.

TABLE I. Characteristics of typical plankters: size d (in mm), swimming velocity V_{swim} (in mm s^{-1}), and reorientation time τ_{align} (in s). The reorientation time depends on the origin of the alignment torque [34]. For surfers, this torque is due to active swimming and $\tau_{\text{align}}^{\text{surf}} = d/(3V_{\text{swim}})$ with d the plankter size. For bottom-heavy swimmers, it is due to gravity and $\tau_{\text{align}}^{\text{b-h}} = 3\nu/(g\delta)$ [40] with g the acceleration of gravity and δ the distance between the center of mass and the geometrical center (we choose $\delta = d/200$, a value typical for zooplankton [41, 42]).

	d	V_{swim}	$\tau_{\text{align}}^{\text{surf}}$	$\tau_{\text{align}}^{\text{b-h}}$
copepod	1	3	0.1	0.008
invertebrate larva	0.2	2	0.03	0.02
dinoflagellate	0.03	0.3	0.03	0.2

Third, the equations of motion given in Eqs. (1) assume an instantaneous reorientation. This assumption would require the plankter to exert an infinitely large torque on the fluid. For a finite torque, the equation of orientation, Eq. (1b), should be replaced by [40]

$$\frac{d\hat{\boldsymbol{p}}}{dt} = \frac{1}{2}\boldsymbol{\omega}(\boldsymbol{X}, t) \times \hat{\boldsymbol{p}} + \frac{1}{2\tau_{\text{align}}}\left[\hat{\boldsymbol{n}} - (\hat{\boldsymbol{n}} \cdot \hat{\boldsymbol{p}})\hat{\boldsymbol{p}}\right], \quad (9)$$

where $\boldsymbol{\omega}(\boldsymbol{x}, t) = \boldsymbol{\nabla} \times \boldsymbol{u}$ is the flow vorticity, and where τ_{align} is a characteristic reorientation time that arises from the balance between the viscous torque and the aligning torque [34]. Figure 4b shows how the performance of surfers ($\hat{\boldsymbol{n}} = \hat{\boldsymbol{n}}_{\text{surf}}$) and bottom-heavy swimmers ($\hat{\boldsymbol{n}} = \hat{\boldsymbol{z}}$) decreases as τ_{align} increases. This loss of performance is essentially due to the flow vorticity, which acts as a noise tilting the swimmer away from its preferred direction. Nevertheless surfers always outperform bottom-heavy swimmers with the same reorientation time. Besides, as long as $\tau_{\text{align}} \lesssim 2\tau_\eta$, the effective speed of surfers V_{eff} remains larger that their swimming speed V_{swim}.

Vertical migration of plankton is essential to ecologically-important activities such as daily migration, dispersal, and larval settlement. Here, we assess the expected benefit of the surfing strategy over bottom-heaviness for vertical migration in different marine habitats. To perform this comparison, we use three typical plankters: a copepod, an invertebrate larva, and a dinoflagellate, whose sizes, velocities and reorientation times are given in Tab. I. The performance of these typical plankters over a wide range of turbulence conditions [43] is shown in Fig. 5. This figure uses empirical fits deduced from our simulations [34] that accounts for the performance drop when $V_{\text{swim}} \gtrsim u_\eta$ or when $\tau_{\text{align}} \gtrsim \tau_\eta$. Although it has been suggested that oceanic turbulence might be weaker than initially thought [38], this figure shows that typical zooplankton species could benefit from the surfing strategy across a wide range of habitats where vertical migration is crucial, in particular
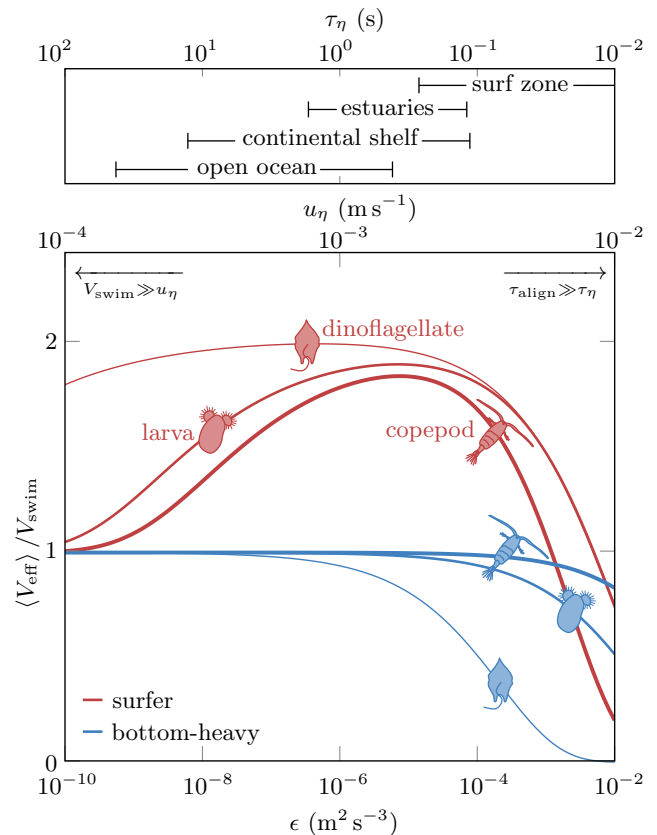

FIG. 5. Expected vertical migration speed (effective vertical velocity, V_{eff}, Eq. (2), relative to swimming velocity V_{swim}) as a function of the turbulence dissipation rate ϵ [34]. We consider three typical plankters: a copepod, an invertebrate larva, and a dinoflagellate, whose characteristics are given in Tab. I. Two strategies are compared: the proposed surfing strategy (red) and bottom-heavy swimmers (blue) orienting upwards due to gravity. In the upper panel, we indicate the range of turbulence intensity for different marine habitats (data from [43]) and the corresponding range of Kolmogorov time τ_η and Kolmogorov velocity u_η, Eq. (6).

continental shelves, estuaries and open oceans.

It is interesting to compare the proposed surfing strategy to agents trained by reinforcement learning. In Ref. [24], a swimming agent was trained to minimize the time to reach a fixed target using a local measure of vorticity in 3D turbulence. We evaluated the performance of this trained agent on our task by placing the target infinitely far and using a similar turbulence level ($Re_\lambda = 21$). For the same swimming parameters ($V_{\text{swim}} = 1.5u_{\text{rms}}$, $\tau_{\text{align}} = 0.5\tau_\eta$), surfers are able to perform 1.5 times better than agents trained by reinforcement learning [34]. Although the comparison remains indicative as reinforcement learning agents were trained with a slightly different objective, it shows that the surfing strategy is performant and should be used as a reference in reinforcement learning problems.

In summary, we have shown that the planktonic navi-

gation problem of going upwards has an approximate analytical solution, which we called surfing. The proposed surfing strategy has three important properties: (1) it is efficient, the effective upward velocity being as large as twice the swimming speed, (2) it is adaptive to different turbulent intensities, (3) and it is robust to finite-time reorientation and various sources of noise. We showed that surfing involves a single adjustable parameter, interpreted as a time horizon and related to the correlation time of the flow gradient seen by the swimmer in turbulence. Finally, we have shown that surfing, which exploits information provided by local velocity gradients, provides a clear benefit over bottom-heaviness for vertical migration of various planktonic species across a wide range of marine habitats.

---

[1] P. Lenz, D. Hartline, J. Purcell, and D. Macmillian, *Zooplankton: sensory ecology and physiology* (CRC Press, 1997).

[2] J. D. Wheeler, E. Secchi, R. Rusconi, and R. Stocker, Annu. Rev. Cell Dev. Biol. **35**, 213 (2019).

[3] T. Kiørboe, E. Saiz, and A. Visser, Mar. Ecol. Prog. Ser. **179**, 97 (1999).

[4] J. Yen, P. H. Lenz, D. V. Gassie, and D. K. Hartline, J. of Plankton R. **14**, 495 (1992).

[5] S. A. Richards, H. P. Possingham, and J. Noye, J. Plankton Res. **18**, 2199 (1996).

[6] C. Adams and A. Paul, J. Crustacean Biol. **19**, 106 (1999).

[7] J. H. Long, A. C. Lammert, C. A. Pell, M. Kemp, J. A. Strother, H. C. Crenshaw, and M. J. McHenry, IEEE J. Oceanic Eng. **29**, 795 (2004).

[8] J. Ringelberg, *Diel vertical migration of zooplankton in lakes and oceans: causal explanations and adaptive significances* (Springer Science & Business Media, 2009).

[9] L. McEdward, *Ecology of marine invertebrate larvae* (CRC press, 2020).

[10] J. Welch and R. Forward, Mar. Biol. **139**, 911 (2001).

[11] M. J. Kingsford, J. M. Leis, A. Shanks, K. C. Lindeman, S. G. Morgan, and J. Pineda, Bull. Mar. Sci. **70**, 309 (2002).

[12] M. G. Hadfield and M. Koehl, Biol. Bull. **207**, 28 (2004).

[13] H. L. Fuchs, L. S. Mullineaux, and A. R. Solow, Limnol. Oceanogr. **49**, 1937 (2004).

[14] H. L. Fuchs, G. P. Gerbi, E. J. Hunter, A. J. Christman, and F. J. Diez, J. Exp. Biol. **218**, 1419 (2015).

[15] H. L. Fuchs, G. P. Gerbi, E. J. Hunter, and A. J. Christ-man, Proc. Natl. Acad. Sci. U.S.A. **115**, E7532 (2018).

[16] J. D. Wheeler, K. R. Helfrich, E. J. Anderson, and L. S. Mullineaux, Limnol. Oceanogr. **60**, 1332 (2015).

[17] E. Zermelo, ZAMM **11**, 114 (1931).

[18] G. Reddy, A. Celani, T. J. Sejnowski, and M. Vergassola, Proc. Natl. Acad. Sci. U.S.A. **113**, E4877 (2016), 27482099.

[19] G. Reddy, J. Wong-Ng, A. Celani, T. J. Sejnowski, and M. Vergassola, Nature **562**, 236 (2018).

[20] S. Colabrese, K. Gustavsson, A. Celani, and L. Biferale, Phys. Rev. Lett. **118**, 158004 (2017).

[21] K. Gustavsson, L. Biferale, A. Celani, and S. Colabrese, **40**, 110 (2017).

[22] J. Qiu, N. Mousavi, K. Gustavsson, C. Xu, B. Mehlig, and L. Zhao, J. Fluid Mech. **932** (2022).

[23] J. Qiu, N. Mousavi, L. Zhao, and K. Gustavsson, "Active gyrotactic stability of microswimmers using hydromechanical signals," (2020), arXiv:2105.12232 [cond-mat, physics:physics].

[24] J. K. Alageshan, A. K. Verma, J. Bec, and R. Pandit, Phys. Rev. E **101**, 043110 (2020).

[25] P. Gunnarson, I. Mandralis, G. Novati, P. Koumoutsakos, and J. O. Dabiri, "Learning Efficient Navigation in Vortical Flow Fields," (2020), arXiv:2102.10536 [physics].

[26] F.-G. Michalec, I. Fouxon, S. Souissi, and M. Holzner, Elife **9**, e62014 (2020).

[27] A. W. Visser, P. Mariani, and S. Pigolotti, J. Plankton Res. **31**, 121 (2009).

[28] M. A. R. Koehl, J. A. Strother, M. A. Reidenbach, J. R. Koseff, and M. G. Hadfield, Mar. Ecol. Prog. Ser. **335**, 1 (2007).

[29] M. Koehl and T. Cooper, ICB **55**, 683 (2015).

[30] N. Pujara, M. Koehl, and E. Variano, J. Fluid Mech. **838**, 356 (2018).

[31] D. Grünbaum and R. R. Strathmann, J. Mar. Res. **61**, 659 (2003).

[32] C. B. Woodson, D. R. Webster, M. J. Weissburg, and J. Yen, Integr. Comp. Biol. **47**, 831 (2007).

[33] U. Frisch and A. Kolmogorov, *Turbulence: the legacy of AN Kolmogorov*.

[34] See Supplemental Material for additional details and results, which also includes [43–47].

[35] Y. Li, E. Perlman, M. Wan, Y. Yang, C. Meneveau, R. Burns, S. Chen, A. Szalay, and G. Eyink, J. Turbul. , N31 (2008).

[36] E. Perlman, R. Burns, Y. Li, and C. Meneveau, in *Proceedings of the 2007 ACM/IEEE conference on Supercomputing* (2007) pp. 1–11.

[37] Our in-house code is available at `http://www.github.com/COPEPOD/sheldOn`.

[38] P. J. Franks, B. G. Inman, J. A. MacKinnon, M. H. Alford, and A. F. Waterhouse, Limnol. Oceanogr. **67**, 348 (2022).

[39] H. Yu and C. Meneveau, Phys. Rev. Lett. **104**, 084502 (2010).

[40] T. J. Pedley and J. O. Kessler, Annu. Rev. Fluid Mech. **24**, 313 (1992).

[41] P. R. Jonsson, Mar. Ecol. Prog. Ser. **52**, 39 (1989).

[42] D. Fields and J. Yen, J. Plankton Res. **19**, 79 (1997).

[43] H. L. Fuchs and G. P. Gerbi, Prog. Oceanogr. **141**, 109 (2016).

[44] H. Lamb, New York **43** (1945).

[45] G. G. Stokes *et al.*, (1851).

[46] G. Lesur and P.-Y. Longaretti, A & A **444**, 25 (2005).

[47] G. Lesur and P.-Y. Longaretti, MNRAS **378**, 1471 (2007).